

Japanese cedar (*Cryptomeria japonica*) ash as a natural activating agent for preparing activated carbon

Chia-Wen Peng · Han Chien Lin

Received: 28 July 2014 / Accepted: 12 December 2014 / Published online: 4 February 2015
© The Japan Wood Research Society 2015

Abstract Japanese cedar (*Cryptomeria japonica*) ash was used as a natural activating agent and also a precursor to prepare activated carbon (AC) using various ash to water ratios (0.20, 0.25, and 0.33 wt%), activation temperatures (750, 850, and 950 °C), and activation durations (0.5, 1.0, and 1.5 h). The yields, iodine value, and methylene blue adsorption value of Japanese cedar AC were in the ranges of 27.3–30.7 %, 953.5–1150.9, and 695.1–1368.0 mg/g. As the ash to water ratio increased, the BET specific surface area and total pore volume of the AC increased. Japanese cedar AC prepared using an ash to water ratio of 0.33 wt%, an activation temperature of 850 °C, and an activation duration of 1.0 h exhibited the highest BET specific surface area (1430 m²/g) and total pore volume (0.74 cm³/g). The nitrogen adsorption–desorption isotherms of the Japanese cedar AC were classified as type IV, indicating the presence of microporous and mesoporous structures, according to the Bruauer, Deming, Deming, and Teller classification. Therefore, Japanese cedar ash with a suitable ash to water ratio can serve as an excellent natural activating agent for preparing AC because a high BET specific surface area can be obtained.

Keywords Japanese cedar ash · Activated carbon · Ash to water ratio · Natural activating agent

Introduction

Activated carbon (AC) is generally regarded as a porous material that has a large specific surface area, a high adsorption capacity, chemical stability, and the ability to regenerate through desorption. Therefore, AC is widely used as an adsorbent for separating and purifying gaseous or aqueous solution systems as a catalyst supporter, or for recovering precious metals [1–3]. Two methods are commonly used for preparing AC: physical and chemical activation. Physical activation consists of two different steps, i.e. carbonization and subsequent partial gasification of the raw material (precursor) with steam, air or CO₂, usually at high temperature (800–1000 °C) [1–3]. In chemical activation, carbonization and activation proceed simultaneously and at a much lower temperature (450–700 °C) in the presence of an activating agent. The activating agents are dehydrating agents, which influence the pyrolytic decomposition of the precursor and inhibit tar formation [1, 2]. Furthermore, many types of activating agents exist, such as H₃PO₄, K₂CO₃, ZnCl₂, and KOH [4–8]. These agents are generally strong acids or alkalis, or substances containing alkali metals. Among the chemical activating agents, ZnCl₂ and H₃PO₄ are typically used for preparing AC [4, 5] through the corrosion, dissolution, or dehydration of precursors; moreover several agents oxidize precursors. Chemical activation requires a lower activation temperature and a shorter activation duration than does physical activation, and can be used to obtain an excellent pore structure and high carbon yield [2]. In the United States, most AC (40–50 %) is prepared using chemical

C.-W. Peng
Ph. D Program of Agriculture Science, College of Agriculture,
National Chiayi University, 300 University Rd., Chiayi 60004,
Taiwan

C.-W. Peng
Experimental Forest, College of Bio-Resources and Agriculture,
National Taiwan University, Nantou, Taiwan

H. C. Lin (✉)
Department of Wood Based Materials and Design, National
Chiayi University, NCYU, 300 University Rd., Chiayi 60004,
Taiwan
e-mail: alexhlin@mail.ncyu.edu.tw

activation, but the environmental pollution, eutrophication, equipment corrosion, and residual activating agent in the AC remain serious problems [9, 10]. Therefore, developing another suitable activating agent for industrially preparing AC is critical, and natural materials are considered to be excellent choices for this purpose.

In recent years, because of the rising price of petroleum and natural gas, and the threat of increasing greenhouse gases, wood pellets have attracted considerable attention [11]. Wood pellets are used in large-scale applications, such as industrial heating systems, coal-powered boilers, and heat gasification [12], or in small-scale operations involving district area and household heating systems [13–15]. The wood pellet market is increasing substantially, and more than 442 pellet plants exist in the world, with a total production capacity of 14 million tons a year [14, 16]. Generally, wood pellets are used for energy production, but the large amount of wood pellet ash generated during combustion goes to landfills [17–19] or is used in farmland or forest fertilization and soil improvement because of its nutrient and trace element content, and acid neutralization capacity [18, 20–29]. However, wood ash does not improve tree growth or biomass production because of its low nitrogen content, and causes biomass to decrease slightly [21, 23–25]; furthermore, it is strongly alkaline (pH 13.3) and contains several metal salts, oxides, hydroxides, and carbonates [28, 30]. According to Marsh and Rodríguez-Reinoso [31], the mechanism for preparing AC involves alkali salt activation, in which the oxygen atoms of hydroxide and potassium or sodium carbonate gasify carbon atoms to produce CO gas, thereby creating porosity. This gasification is catalyzed by the alkali metal salt. The reduction of an alkali metal salt produces potassium or sodium metal atoms, which are intercalated into the carbon structure, thereby expanding the carbon matrix [4, 5, 7, 32–34].

The Taiwanese government has strongly encouraged afforestation, using species such as *Cunninghamia lanceolata*, *Cryptomeria japonica*, and *Taiwania cryptomerioides*. The plantation growing stock is now over 30 years old, and has not been subjected to thinning, particularly Japanese cedar, which has currently reached 23,000 ha with approximately 4 million m³ of wood. Implementing massive thinning is essential to obtain optimal tree growth, because thinning produces logs with a small diameter utilization and generates approximately 3.6×10^5 m³ of woody biomass residues [35]. Japanese cedar is a suitable precursor for preparing charcoal [35, 36], bio-charcoal [37] and a potential material for producing wood pellets [19, 38, 39]. In addition, Japanese cedar wood is suitable for preparing AC because of its high carbon content and low cost [2, 8, 40–42]. Extensive research has been conducted to investigate the applications of wood pellet ash in farmland

and forest fertilization or soil improvement [18, 20–29]; however, new applications are rare. In this study, Japanese cedar ash was used as a natural activating agent to prepare AC from the thinning wood of Japanese cedar and also as a precursor under diverse conditions; specifically, the activation temperature, activation duration, and ash to water ratios. The yield, iodine value, methylene blue adsorption value, BET specific surface area, and porosity characteristics of the AC were investigated. The results can be used as a reference for using the ash of wood pellets after combustion, and can also be used as an example of an activation method for preparing AC to implement the sustainable reuse of resources.

Materials and methods

Materials

A Japanese cedar (*Cryptomeria japonica* D. Don) tree, used to obtain the precursor material, was obtained from the Experimental Forest at the College of Bio-Resources and Agriculture, National Taiwan University in Nantou County, Taiwan. The tree was approximately 40 years old, and the average specific gravity was approximately 0.41. The tree was debarked, crushed and sieved to obtain particles with a size between 0.38 and 0.83 mm [43]. To obtain wood ash, the thinned wood log (with a dimension of approximately 20–30 cm) was stacked on an iron grid and burned. The wood ash was then collected to be used as a natural activating agent, and sieved to remove dust before preparing the AC.

Preparing wood ash–water mixture with different ratio

Japanese cedar wood ash and distilled water were mixed using various weight proportions, boiled for 10 min, and filtered to obtain various ash to water ratios (0.20, 0.25, and 0.33 wt%). The sample codes were JC-0.20, JC-0.25, and JC-0.33. The pH value of the wood ash–water mixture was tested using a pH meter (Suntex TS-1).

Preparation of activated carbon

The precursor and wood ash–water mixture were mixed, impregnated for 24 h, and filtered. The mixture was heated in an oven at 105 °C for 24 h. The weight gains of the precursors JC-0.20, JC-0.25, and JC-0.33 were approximately 7.6, 17.2, and 23.2 %, respectively. The resulting mixture and the sample in the control group (without wood ash–water mixture impregnation) were loaded in a crucible, which was placed inside an upright high-temperature activation furnace (inner diameter, 26 cm; inner height,

40 cm). Each sample was heated under a nitrogen flow (200 mL/min) for carbonization at a rate of 10 °C/min, and maintained at the desired temperature for 0.5, 1.0, and 1.5 h. The activation temperature was set at 750, 850, and 950 °C [4, 5, 34]. The sample code was Japanese cedar wood ash (JC)–ash to water ratio–activation temperature–activation duration. After cooling the furnace to room temperature under the nitrogen flow [4, 5, 7, 34], the AC was washed with a 1 N HCl solution, stirred for 30 min to leach out the activating agent, and washed repeatedly with distilled water at 90 °C to remove excess acid until the pH value of the washed solution was approximately 6–7 [44, 45]. Subsequently, the AC was dried in the oven at 105 °C for 24 h.

Basic properties of Japanese cedar wood

Japanese cedar particles were washed with distilled water to remove dust, dried for 24 h at 105 °C to reduce the moisture content, and grounded to obtain fine particles with sizes less than 0.25 mm.

The carbon (C), hydrogen (H), nitrogen (N), oxygen (O), and sulfur (S) contents of the Japanese cedar particles were determined using an elemental analyzer (Elemental Vario CHNS/O Analyzer, EA, Germany).

Proximate analysis was conducted according to Chinese National Standard (CNS) 10821 [46], CNS 10822 [47], CNS 10823 [48], and CNS 10824 [49]. The results regarding moisture, ash, volatile matter, and fixed carbon content were subsequently obtained.

Thermogravimetric analyses (TGA) were conducted using a thermogravimetric analyzer (Perkin Elmer Pyris1) to determine the pyrolysis behavior of both the Japanese cedar wood and the wood impregnated by wood ash–water mixture at various ash to water ratios. A sample weighing approximately 5.0–10.0 mg was placed on the tray of the analyzer and heated at a temperature range of 25–850 °C, with a heating rate of 10 °C/min, under a nitrogen flow at a rate of 100 mL/min.

Characterization of wood ash

The pH value of Japanese cedar wood ash was determined according to CNS 697 (1965) [50]. A sample weighing 10 mg was placed on a flask equipped with a boiler-reflux condenser, and 30 mL of distilled water was added to the flask and boiled for 5 min. Finally, the supernatant liquid was determined using a pH meter after cooling the mixture to room temperature.

Inductively coupled plasma-optical emission spectroscopy (ICP-OES) was conducted using an ULTIMA 2000 (Horiba Jobin–Yvon) to determine the content of Si, Al,

Na, K, Mg, Ca, Ti, and Fe of wood ash. Briefly, ash and co-solvent (3 mg of lithium carbonate and 10 mg of boric acid) were weighed and mixed thoroughly. The sample was transferred into a platinum crucible to be burnt at 1000 °C, and approximately 9.09 % of nitric acid was added. Finally, the content of trace elements was determined by conducting ICP-OES after ultra-sonication. The wood ash–water mixtures were also measured using ICP-OES after the mixture was diluted with ultra-pure water to a 1 % concentration.

Characterization of activated carbon

The yield of AC (based on a dry basis) was calculated using the following equation:

$$\text{Yield, \%} = \frac{\text{activated carbon, g}}{\text{Japanese cedar wood, g}} \times 100.$$

Iodine value was determined according to JIS K 1474 (1991) [51]. The activated carbon particle size was 40 mesh to 60 mesh, and the equation for determining the iodine adsorption value was $I = (10 - K \times f) \times 12.69 \times 5/M$; (I iodine adsorption value (mg/g); K volume of sodium thiosulfate solution used for titration (mL); f ratio of 0.1 N sodium thiosulfate solution to 0.1 N iodine solution; M absolute dry weight of the sample).

To determine the methylene blue (MB) adsorption value, AC (1 mg) was added to a 25 mL aqueous solution containing 1 g/L of MB, and shaken at room temperature (30 °C). When the aqueous solution became colorless, MB was added into the flask repeatedly to assure the equilibrium adsorption of MB. After filtration, the concentration of residual MB was determined using a UV–vis spectrophotometer (CECIL, CE3041) at a wavelength of 664 nm. This test method was based on that used by Wu et al. [52].

The potassium (K) ions of AC (without acid washing) were determined by applying X-ray fluorescence (XRF) using an XGT-1000WR X-ray fluorescent analyzer (HORIBA).

The pore structure characteristics of the various samples were measured by nitrogen adsorption–desorption isotherms at 77 K using a Micromeritics ASAP 2020 at a relative pressure (P/P_0) ranging from 10^{-2} to 1. BET specific surface area (S_{BET}) was determined using the standard BET equation, applied to a relative pressure range from 0.06 to 0.2. The t -plot and Barret–Joyner–Halenda (BJH) [53] analysis software were used to calculate the external surface area (S_{ex}), micropore volume (V_{mi}), and pore size distribution. The total pore volume (V_{tot}) was estimated as the liquid volume of nitrogen at a high relative pressure of 0.98, and the average pore diameter (D) was calculated using the equation $(4V_{\text{tot}}/S_{\text{BET}}) \times 10^3$ [54].

In addition, the results expressing mean and standard deviation were statistically analyzed by applying Duncan’s multiple range tests at a 5 % significance level, using the Statistical Package for Social Science (SPSS 16.0) software.

Results and discussion

Elemental and proximate analysis

The results of elemental analysis are shown in Table 1. The carbon content of Japanese cedar wood was about 48.96 %. Lin et al. [55] reported that the average carbon content of nine types of conifers was 48.21 %, and Japanese cedar exhibited the highest carbon content (49.03 %). The results of the proximate analysis of Japanese cedar wood are also shown in Table 1. Compared with other woody materials, such as birch, Chinese fir, and bamboo [42, 56, 57], the fixed carbon content of which was between 12.0 and 14.98 %, and the ash content was approximately 0.2–1.22 %, Japanese cedar wood exhibited a high fixed carbon content (16.63 %) and a low ash content (0.22 %). These results suggest that Japanese cedar wood is a suitable precursor for preparing AC.

Thermogravimetric analysis

Thermal analysis (TGA/DTG) of the Japanese cedar wood was performed to examine its decomposition characteristics. Three stages were observed in the TGA curve for Japanese cedar wood (without activation with wood ash): 45–250, 250–380, and 380–850 °C (Fig. 1), representing dehydration, devolatilization, and the consolidation of the char structure, respectively [10, 58]. A sharp weight loss was observed over 250 °C. In the second stage, the specimen registered a sharp weight loss of approximately

60.4 % at the temperature range of 250–380 °C, in which the carbonization process initiated and in which hemicellulose and cellulose fractions were mainly decomposed [3]. The weight losses gradually decreased as the temperature increased from 380 to 850 °C in the final stage. When the decomposition of the chemical components was devolatilized, the weight of the specimen decreased by approximately 81.3 % at the temperature range of 25–850 °C. The curves obtained through the TGA and differential thermogravimetric (DTG) analysis showed that for the three samples impregnated with the wood ash–water mixture of JC-0.20, JC-0.25, and JC-0.33, the peaks of the pyrolysis temperature were 242, 236, and 234 °C, and the corresponding weight losses were 38.96, 36.08, and 46.01 %, respectively. The thermal decomposition behavior

Table 1 Elemental and proximate analyses of Japanese cedar wood

Experimental	Item	Weight (%)
Elemental analysis	Carbon	48.96 (0.11) ^a
	Nitrogen	0.43 (0.12)
	Hydrogen	6.50 (0.03)
	Oxygen ^b	43.65 (0.70)
	Sulfur	0.46 (0.48)
Proximate analysis	Moisture	6.55 (0.13)
	Volatile matter	76.60 (0.09)
	Fixed carbon	16.63 (0.14)
	Ash	0.22 (0.06)

^a () represents standard deviation

^b By difference

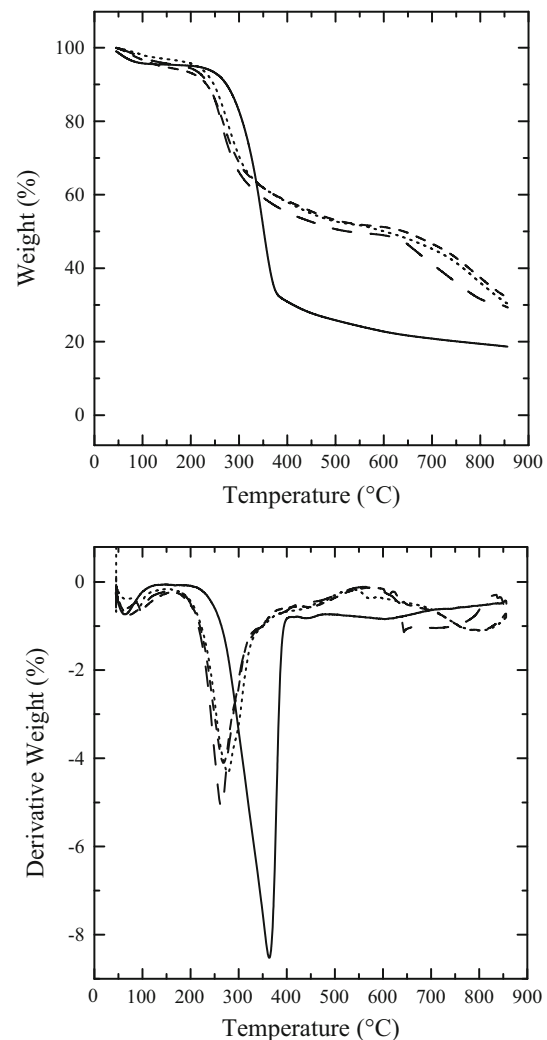


Fig. 1 TGA and DTG curves for Japanese cedar wood and three samples activated with Japanese cedar ash. Legends: — JC-0.00, ····· JC-0.20, - - - - JC-0.25, - · - · JC-0.33. TGA thermogravimetric analyses, DTG differential thermogravimetric, JC Japanese cedar wood ash

changed, and the pyrolysis temperature of the samples decreased with as the ash to water ratio increased. In addition, when the temperature increased to 564, 577, and 540 °C, the weight loss of JC-0.20, JC-0.25, and JC-0.33 gradually increased, respectively. Hayashi et al. [4] prepared AC from various nutshells by chemical activation with K_2CO_3 at temperatures above 627 °C; the carbon in the shell chars was consumed by reducing K_2CO_3 to carbon monoxide, resulting in additional weight loss. Therefore, we deduced that weight loss occurred at temperatures over 540 °C. The Japanese cedar char was consumed through the reduction of K ions in wood ash, resulting in additional weight loss.

Analysis of the activating agent

The pH value of Japanese cedar wood ash was 12.86 (Table 2). Sano et al. [19] reported that the pH value of the ash from Japanese cedar wood pellets used for fuel was 13.2, measured using a leaching test (ash to water ratios = 0.1 wt%). Although the test methods differed, the results were similar. The results of Table 2 also revealed that the pH value of the wood ash–water mixture was between 13.68 and 14.03, and increased when the ash to water ratio increased. In addition, the results of the elemental analysis of Japanese cedar ash and the wood ash–water mixture, obtained using ICP-OES are also given in Table 2. K, Ca, and Mg were the predominant elements in the wood ash. The predominant compounds in the wood ash were K_2O (34.3 %), CaO (34.3 %), MgO (5.75 %), and SiO_2 (3.86 %). These results were the same as the results obtained using ash from Japanese cedar wood pellets used for fuel. In Sano et al. [19], K (160 g/kg) and Ca (180 g/kg) were the predominant elements, followed by Si (40 g/kg) and Mg (34 g/kg). In addition, the highest concentration of K was observed in the wood ash–water mixture, which was between 47832.4 and 72509.0 ppm, and was also related to the ash to water ratio. However, K_2O dissolved in the

mixture of wood ash–water more easily than CaO did because the predominant compound in K_2O was water-soluble potassium (approximately 90 %). Thus, the concentration of Ca was between 2.9 and 4.8 ppm, which was lower than that of K.

Characterization of activated carbon

As shown in Table 3, the yields of the sample in the control group (without wood ash–water mixture impregnation) ranged from 25.1 to 25.7 % for Japanese cedar char prepared at carbonization temperatures of 750, 850, and 950 °C and a carbonization duration of 1.0 h. The results revealed that the difference in the carbon yield was not significant (5 %), in accordance with Duncan's multiple range tests. In addition, the iodine value and MB value ranged from 156.0 to 337.0 mg/g and from 0.6 to 13.5 mg/g, respectively. The highest iodine value (337.0 mg/g) was obtained at a carbonization temperature of 850 °C, and the difference in the iodine value of the chars was significant. Moreover, the AC yields ranged from 27.3 to 30.7 % when using ash activation. Guo and Lua [33] prepared AC from palm shell using potassium hydroxide impregnation at various stages. The impregnation of the raw palm shell was achieved by replacing a fraction of the hydrogen ions with potassium (K) ions, and forming cross-linked complexes. The presence of potassium hydroxide in the interior of the precursor restricted the formation of tar and other liquids such as acetic acid and methanol, which are produced during the carbonization process, resulting in a relatively high yield compared with that produced by the process without impregnation. Therefore, the AC produced by wood ash activation produced higher yields than those of the sample in the control group (Table 3). We deduced that the presence of K ions (Tables 2, 3) derived from the Japanese cedar wood ash in the interior of the precursor slowed down the formation of tar and other liquids by forming cross-links, thus resulting in an increased yield.

Table 2 pH values and elemental analysis of Japanese cedar wood ash and Japanese cedar wood ash–water mixture

Sample	pH	Ash analysis (% oxides)								
		SiO_2	Al_2O_3	Na_2O	K_2O	MgO	CaO	TiO_2	Fe_2O_3	
Ash	12.86	3.86	0.75	ND	34.30	5.75	34.30	0.05	0.79	
Ash–water mixture	pH	Ash–water analysis (ppm)								
		Si	Al	Na	K	Mg	Ca	Ti	Fe	
JC-0.20		13.68 (0.01)	317.4	4.7	312.1	47832.4	0.1	2.9	0.2	0.1
JC-0.25		13.80 (0.02)	367.5	2.2	394.4	60788.3	ND	3.1	0.2	0.2
JC-0.33		14.03 (0.04)	573.9	8.1	509.4	72509.0	0.4	4.8	0.3	0.3

ND not detected

Table 3 Yield, iodine value, methylene blue adsorption value, and K ions content of ACs prepared under various conditions

Sample identification code	Yield (%)	Iodine value (mg/g)	MB ³ (mg/g)	K ions ⁴ (wt%)
0-750-1.0 ¹	25.4 (0.6) ^{a 2}	203.0 (8.0) ^b	2.3 (0.8) ^b	0.40 (0.03) ^a
0-850-1.0	25.1 (0.8) ^a	337.0 (25.0) ^c	13.5 (0.9) ^c	0.88 (0.04) ^b
0-950-1.0	25.7 (0.2) ^a	156.0 (7.0) ^a	0.6 (0.4) ^a	1.74 (0.02) ^c
JC-0.33-750-1.0	30.7 (1.1)	953.5 (3.9)	836.9 (18.9)	12.87 (0.09)
JC-0.20-850-1.0	27.3 (0.7)	1055.9 (37.5)	695.1 (28.2)	11.45 (0.09)
JC-0.25-850-1.0	28.4 (0.9)	1097.4 (16.3)	1012.1 (32.1)	12.45 (0.13)
JC-0.33-850-0.5	30.4 (0.7)	1150.9 (7.8)	1010.6 (44.6)	13.10 (0.21)
JC-0.33-850-1.0	29.1 (0.6)	1106.4 (12.9)	1108.0 (20.4)	12.60 (0.20)
JC-0.33-850-1.5	28.3 (0.5)	1093.8 (3.3)	1023.5 (33.9)	11.65 (0.14)
JC-0.33-950-1.0	28.0 (0.2)	1121.4 (15.4)	1368.0 (30.3)	6.10 (0.12)

¹ Sample identification code: ash (JC)–ash to water ratio–activation temperature–activation duration

² Mean (standard deviation) separation within columns by Duncan's multiple range tests at a 5 % significance level for yield, iodine value, MB, and K ions. Repeated letters indicate no significant differences between two variable factors, whereas significant differences are expressed by the use of different letters (a–c)

³ MB: methylene blue adsorption value

⁴ K ions: samples without acid washing were measured using XRF

However, the activation temperature and reaction duration strongly influenced the yield. The results of Table 3 obtained that the iodine value and MB values of the AC prepared using wood ash activation ranged from 953.5 to 1150.9 mg/g and from 695.1 to 1368.0 mg/g, respectively; these values were higher than those of the sample in the control group (which registered iodine and MB values of 156.0–203.0 and 0.6–13.5 mg/g, respectively). The iodine value (953.5–1121.4 mg/g) and MB value (695.1–1108.0 mg/g) increased with either the activation temperature (750–950 °C) or ash to water ratio (0.20–0.33 wt%), respectively. JC-0.33-850-0.5 exhibited the highest iodine value (1150.9 mg/g), and JC-0.33-950-1.0 exhibited the highest MB value (1368.0 mg/g). The iodine value denotes the amount of micropores, whereas the MB value can be used to estimate the capability of AC for adsorbing large organic molecules [59], and indicates the amount of mesopores in the AC [3]. Commercial ACs produce iodine values normally ranging from 600 to 1000 mg/g [52]. Therefore, the iodine values of the ACs prepared using wood ash activation were similar to the commercial value.

K ions content

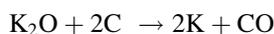
The K ions content in the Japanese cedar char and AC (without acid washing) was determined using XRF. Table 3 shows that the K ions content in Japanese cedar char was between 0.40 % and 1.74 %. The K ions content increased with as the activation temperature increased, and the difference in the K ions content of the sample in the control group (without impregnated with ash–water

mixture) was significant (5 %). However, the K ions content in ACs prepared using wood ash activation ranged from 6.10 to 13.10 %, and was higher than that of the sample in the control group. When using an activation temperature of 850 °C with a duration time of 1.0 h, the K ions content increased as the ash to water ratio and iodine value increased (Table 3). This occurred because the oxygen atoms of the alkali metal salt in wood ash gasify carbon atoms to produce CO gas and produced porosity. Thus, the alkali metal salt of wood ash may play a role as a catalyzer [31]. Hayashi et al. [4] studied that ACs were prepared from various nutshells by activating K₂CO₃, and the carbon in the shell chars was gasified through the reduction of K₂CO₃ to form carbon monoxide. The specific surface area and pore volume of the shell AC increased at activation temperatures higher than 627 °C. Table 3 also shows that at an ash to water ratio below 0.33 wt% and activation temperatures from 750 to 850 °C, the K ions content decreased slightly from 12.87 to 12.60 %. A previous study reported that AC is derived from lignin by activating K₂CO₃. The results of the recovery ratios of K₂CO₃ over the temperature range of 500–900 °C were also presented. The recovery ratio decreased slightly with an increase in temperature, indicating that K₂CO₃ is reduced by carbon in inert atmospheres [32]. However, in this study, the amount of K ions decreased dramatically to 6.10 % at an activation temperature of 950 °C. The melting point of K₂CO₃ was 891 °C [4], and temperatures greater than 900 °C resulted in evaporation. Thus, we deduced that the content of K ions decreased dramatically at the activation temperature of 950 °C; some of the K ions were reduced by carbon and the rest were vaporized.

BET specific surface area and porosity

The S_{BET} and pore characteristics of ACs from Japanese cedar wood ash activated under various conditions are shown in Table 4. The S_{BET} , S_{ex} and V_{tot} increased as the ash to water ratio increased at an activation temperature of 850 °C. JC-0.33-850-1.0 exhibited the highest values, with a S_{BET} , S_{ex} , and V_{tot} of 1430, 707 m²/g, and 0.74 cm³/g. The optimal S_{BET} and porosity can be obtained using an activation duration of 1.0 h. However, with an activation temperature of 950 °C (JC-0.33-950-1.0), the S_{BET} decreased from 1430 to 1345 m²/g, the S_{ex} decreased from 707 to 631 m²/g, and the V_{tot} decreased from 0.74 to 0.68 cm³/g. We deduced that an increase in the activation temperature resulted in a collapse of the internal walls of the micropores or the combination of micropores, creating large pores, and thus decreasing the S_{BET} and V_{tot} of the AC. The activation temperature and ash to water ratio significantly affected the S_{BET} and porosity of AC. An AC with S_{BET} that ranged from approximately 850 to 1430 m²/g was prepared by activation with Japanese cedar wood ash. Such high surface areas were similar to commercial AC values, which range from 500 to 2000 m²/g [60]. Furthermore, as shown in Tables 2, 3, and 4, the K ions content substantially increased as the ash to water ratio increased, which produced a high iodine value, MB value, S_{BET} , S_{ex} , and V_{tot} of AC. In other words, the development of micropores is due to the intercalation of K ions in the carbon structure [7]. Besides, Adinata et al. [34] used palm shells to prepare AC using K₂CO₃. The K ions may intercalate and expand the inter-layers of adjacent hexagonal network planes composed of carbon atoms, thereby increasing pore formation. In this study, the pore structure of AC was formed by activating Japanese cedar wood ash. The potassium compound formed during the activation step diffused into the internal structure of the char matrix, widened the existing pores and created new porosities. The

activation was conducted according to the reaction [4, 5, 61–63] shown in the following equation:



Therefore, we deduced that the development of porosity was catalyzed by the alkali metal salt of wood ash; in addition, the activation process was strengthened by increasing the ash to water ratio. Pore formation was thus enhanced because the K ions contained in the ash intercalated and enlarged the carbon matrix.

Nitrogen adsorption–desorption isotherms and pore size distribution

Figure 2 shows the nitrogen adsorption–desorption isotherms of the ACs prepared using three activation temperatures (750, 850, and 950 °C), an ash to water ratio of 0.33 wt%, and an activation duration of 1.0 h. When the relative pressure P/P_0 value was near 0, the quantity of N₂ adsorbed at 750, 850, and 950 °C was 212, 294, and 279 cm³/g. The quantity of N₂ adsorbed by JC-0.33-750-1.0 exhibited no considerable differences when the P/P_0 value ranged from the minimal to maximal value. The AC obtained was defined as type I, in accordance with the Brunauer, Deming, Deming, and Teller (BDDT) classification based on the type of adsorption isotherm [64]. The major uptake occurred at low relative pressures (less than 0.1), and the predominant microporous materials exhibited a narrow pore size distribution (Fig. 3). The isotherms of JC-0.33-850-1.0 and JC-0.33-950-1.0 exhibited a well-defined plateau and hysteresis loop, and both the hysteresis loop and adsorption “tail” were obvious at a high relative pressure (P/P_0). According to the BDDT classification, these ACs were type IV, indicating the micro-mesopore content of the adsorbents. The pore size distribution of the ACs is shown in Fig. 3. As the activation temperature increased to 850 °C, the amount of micropores and the mesopores increased

Table 4 Porosity of AC prepared under various conditions

Sample identification code	S_{BET} (m ² /g)	t -plot		V_{tot} (cm ³ /g)	$V_{\text{mi}}/V_{\text{tot}}$ (%)	D (nm)
		S_{ex} (m ² /g)	V_{mi} (cm ³ /g)			
JC-0.33-750-1.0 ^a	835	128	0.33	0.41	80.6	1.95
JC-0.20-850-1.0	1061	318	0.34	0.52	66.0	1.96
JC-0.25-850-1.0	1242	463	0.36	0.62	57.8	2.00
JC-0.33-850-0.5	1103	202	0.42	0.53	78.9	1.92
JC-0.33-850-1.0	1430	707	0.33	0.74	44.1	2.08
JC-0.33-850-1.5	1148	317	0.38	0.56	68.4	1.95
JC-0.33-950-1.0	1345	631	0.33	0.68	48.0	2.01

S_{BET} specific surface area, S_{ex} external surface area, V_{mi} micropore volume, V_{tot} total pore volume, D average diameter of pore

^a Sample identification code: ash (JC)–ash to water ratio–activation temperature–activation duration

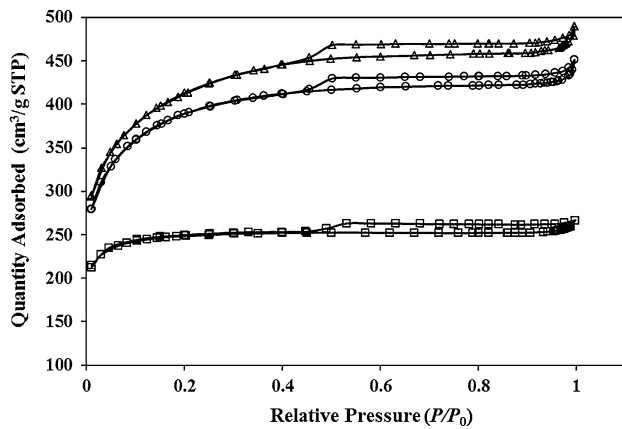


Fig. 2 Nitrogen adsorption–desorption isotherms at 77 K for ACs prepared using various activation temperatures and an ash to water ratio of 0.33 wt%. Legends: \square JC-0.33-750-1.0, \triangle JC-0.33-850-1.0, \circ JC-0.33-950-1.0. ACs activated carbons, JC Japanese cedar wood ash

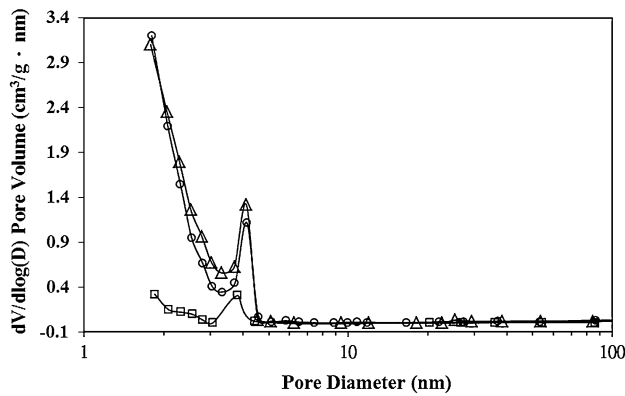


Fig. 3 Pore size distribution of ACs prepared using various activation temperatures and an ash to water ratio of 0.33 wt%. Legends: \square JC-0.33-750-1.0, \triangle JC-0.33-850-1.0, \circ JC-0.33-950-1.0. ACs activated carbons, JC Japanese cedar wood ash

drastically, indicating the creation of a microporous structure and the growth of micropores to mesopores. The creation of mesopores is known to be enhanced by an increase in the activation temperature. Activation temperatures of 850 and 950 °C resulted in an obvious peak with a pore diameter of 4.1 nm (Fig. 3), proving that ACs produced at activation temperatures above 850 °C contained both microporous and mesoporous structures.

To determine the effect of the ash to water ratio on porosity, ACs were prepared using an activation temperature of 850 °C and an activation duration of 1.0 h. The N₂ adsorption–desorption isotherms and pore size distributions of the ACs prepared using various ash to water ratios are shown in Figs. 4 and 5. All the ACs exhibited the hysteresis loop. As the ash to water ratio increased, the knee of the isotherm became increasingly rounded, indicating that

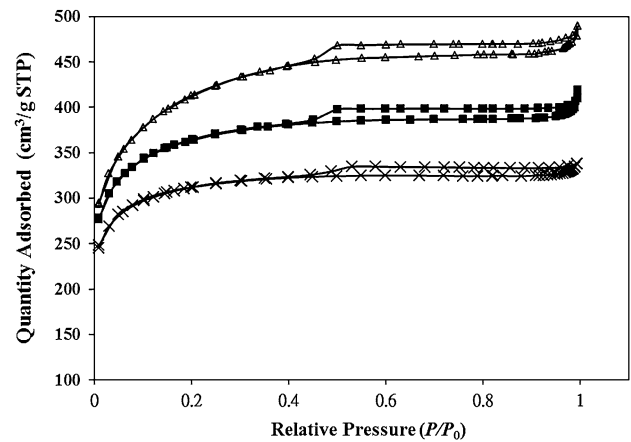


Fig. 4 Nitrogen adsorption–desorption isotherms at 77 K for ACs prepared using various ash to water ratios and an activation temperature of 850 °C. Legends: \times JC-0.20-850-1.0, \blacksquare JC-0.25-850-1.0, \triangle JC-0.33-850-1.0. ACs activated carbons, JC Japanese cedar wood ash

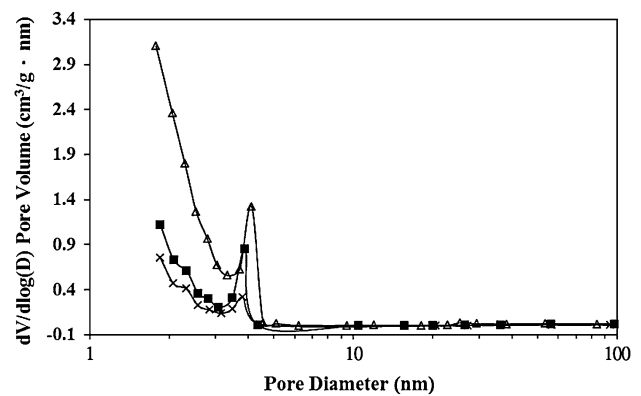


Fig. 5 Pore size distribution of ACs prepared using various ash to water ratios and an activation temperature of 850 °C. Legends: \times JC-0.20-850-1.0, \blacksquare JC-0.25-850-1.0, \triangle JC-0.33-850-1.0. ACs activated carbons, JC Japanese cedar wood ash

both the N₂ adsorption and the V_{tot} increased (Table 4). The pore structure of the produced ACs mainly consisted of micropores when the ash to water ratio was below 0.25 wt% (Fig. 5; Table 4). The ratio of micropore volume to total pore volume (V_{mi}/V_{tot}) was between 57.8 and 66.0 %. The average pore diameter (D) was between 1.96 nm and 2.00 nm. However, when the ash to water ratio increased to 0.33 wt%, the V_{mi}/V_{tot} decreased to 44.1 %, and the D increased to 2.08 nm, demonstrating the formation of a microporous structure and the widening of micropores to mesopores. According to the prior statement, K ions function as catalysts during char gasification and are intercalated into the carbon matrix, resulting in the increase and enlargement of pores through merging, which clearly reflects the considerable effects of the ash to water ratio on the pore structure of AC.

Conclusions

The thinning wood of Japanese cedar was used as the precursor to prepare AC, using Japanese cedar ash as the natural activating agent. The pH value of Japanese cedar ash was 12.86, and its CaO, K₂O, and MgO contents were 34.3, 34.3, and 5.75 %. Japanese cedar wood exhibited a high fixed carbon content of 16.63 % and a low ash content of 0.22 %, indicating that this precursor was suitable for preparing AC. The yield (27.3–30.7 %), iodine value (1055.9–1106.4 mg/g), and MB value (695.1–1108.0 mg/g) of the AC increased as the ash to water ratio increased. An increase in the ash to water ratio also resulted in an increase in the S_{BET} , S_{ex} , and V_{tot} of the AC. The AC prepared using an ash to water ratio of 0.33 wt%, an activation temperature of 850 °C and an activation duration of 1.0 h exhibited the highest S_{BET} (1430 m²/g), S_{ex} (707 m²/g), and V_{tot} (0.74 cm³/g), and its nitrogen adsorption–desorption isotherm was classified as type IV, indicating the presence of micro- and mesoporous structures. Hence, the results indicated that Japanese cedar wood ash with a suitable ash to water ratio can serve as a natural activating agent for preparing AC.

Acknowledgments Fund for this study was provided by the Experimental Forest of National Taiwan University (100 A05).

References

- Manocha SM (2003) Porous carbons. *Sādhanā* 28:335–348
- Yorgun S, Vural N, Demiral H (2009) Preparation of high-surface area activated carbons from paulownia wood by ZnCl₂ activation. *Microporous Mesoporous Mater* 122:189–194
- Sun K, Jiang JC (2010) Preparation and characterization of activated carbon from rubber-seed shell by physical activation with steam. *Biomass Bioenergy* 34:539–544
- Hayashi J, Horikawa T, Takeda I, Muroyama K, Ani FN (2002) Preparing activated carbon from various nutshells by chemical activation with K₂CO₃. *Carbon* 40:2381–2386
- Hayashi J, Horikawa T, Muroyama K, Gomes VG (2002) Activated carbon from chickpea husk by chemical activation with K₂CO₃: preparation and characterization. *Microporous Mesoporous Mater* 55:63–68
- Corcho-Corral B, Olivares-Marín M, Fernández-González C, Gómez-Serrano V, Macías-García A (2006) Preparation and textural characterisation of activated carbon from vine shoots (*Vitis vinifera*) by H₃PO₄—chemical activation. *Appl Surf Sci* 252:5961–5966
- Sudaryanto Y, Hartono SB, Irawaty W, Hindarso H, Ismadji S (2006) High surface area activated carbon prepared from cassava peel by chemical activation. *Bioresour Technol* 97:734–739
- Qiu KQ, Yang SW, Yang J (2009) Characteristics of activated carbon prepared from Chinese fir sawdust by zinc chloride activation under vacuum condition. *J Cent South Univ Technol* 16:385–391
- Tsai WT, Chang CY, Wang SY, Chang CF, Chien SF, Sun HF (2001) Preparation of activated carbons from corn cob catalyzed by potassium salts and subsequent gasification with CO₂. *Bioresour Technol* 78:203–208
- Chang CF, Chang CY, Shie JL, Lee SL, Wang SY, Lin PS, Tsai WT (2003) Production of activated carbons from agricultural waste corn cob by chemical and/or physical activations: an overview. *J Chin Inst Environ Eng* 13:135–141
- Komata H, Orihashi K, Ishikawa Y, Hitoie K, Hattori N (2010) Life cycle impact assessment of wood pellets made in Hokkaido (in Japanese with English abstract). *J Wood Sci* 56:139–148
- Nilsson D, Bernesson S, Hansson PA (2011) Pellet production from agricultural raw materials—a systems study. *Biomass Bioenergy* 35:679–689
- Ståhl M, Wikström F (2009) Swedish perspective on wood fuel pellets for household heating : a modified standard for pellets could reduce end-user problems. *Biomass Bioenergy* 33:803–809
- Ståhl M, Berghel J (2011) Energy efficient pilot-scale production of wood fuel pellets made from a raw material mix including sawdust and rapeseed cake. *Biomass Bioenergy* 35:4849–4854
- Lee YW, Ryu C, Lee WJ, Park YK (2011) Assessment of wood pellet combustion in a domestic stove. *J Mater Cycles Waste Manag* 13:165–172
- Ljungblom L (2007) The Pellets Map 2007—the discussion. *Bioenergy Int* 29:6
- Pitman RM (2006) Wood ash in forestry—a review of the environmental impacts. *Forestry* 79:563–588
- Karlton E, Saarsalmi A, Ingerslev M, Mandre M, Andersson S, Gaitnieks T, Ozolinčius R, Varnagiryte-Kabasinskiene I (2008) Wood ash recycling possibilities and risks. In: Röser D, Asikainen A, Raulund-Rasmussen K, Stupak I (eds) Sustainable use of forest biomass for energy: a synthesis with focus on the Baltic and Nordic region. Springer, The Netherlands, pp 79–108
- Sano T, Miura S, Furusawa H, Kaneko S, Yoshida T, Nomura T, Ohara S (2013) Composition of inorganic elements and the leaching behavior of biomass combustion ashes discharged from wood pellet boilers in Japan. *J Wood Sci* 59:307–320
- Krejzl JA, Scanlon TM (1996) Evaluation of beneficial use of wood-fired boiler ash on oat and bean growth. *J Environ Qual* 25:950–954
- Staples TE, Rees KCJV (2001) Wood/sludge ash effects on white spruce seedling growth. *Can J Soil Sci* 81:85–92
- Arvidsson H, Lundkvist H (2003) Effects of crushed wood ash on soil chemistry in young Norway spruce stands. *For Ecol Manage* 176:121–132
- Jacobson S (2003) Addition of stabilized wood ashes to Swedish coniferous stands on mineral soils—effects on stem growth and needle nutrient concentrations. *Silva Fenn* 37:437–450
- Saarsalmi A, Mälkönen E, Kukkola M (2004) Effect of wood ash fertilization on soil chemical properties and stand nutrient status and growth of some coniferous stands in Finland. *Scand J Forest Res* 19:217–233
- Park BB, Yanai RD, Sahn JM, Lee DK, Abrahamson LP (2005) Wood ash effects on plant and soil in a willow bioenergy plantation. *Biomass Bioenergy* 28:355–365
- Ozolinčius R, Buožytė R, Varnagiryte-Kabašinskiene I (2007) Wood ash and nitrogen influence on ground vegetation cover and chemical composition. *Biomass Bioenergy* 31:710–716
- Adler A, Dimitriou I, Aronsson P, Verwijst T, Weih M (2008) Wood fuel quality of two *Salix viminalis* stands fertilized with sludge, ash and sludge-ash mixtures. *Biomass Bioenergy* 32:914–925
- Nurmesniemi H, Pöykiö R, Kuokkanen T, Rämö J (2008) Chemical sequential extraction of heavy metals and sulphur in bottom ash and fly ash from a pulp and paper mill complex. *Waste Manag Res* 26:389–399
- Mandre M, Pärn H, Klõšeiko J, Ingerslev M, Stupak I, Kört M, Paasrand K (2010) Use of biofuel ashes for fertilization of *Betula pendula* seedlings on nutrient-poor peat soil. *Biomass Bioenergy* 34:1384–1392

30. Kuokkanen M, Pöykiö R, Kuokkanen T, Nurmesniemi H (2009) Wood ash—a potential forest fertilizer. In: Energy Research at the University Oulu Proceedings of the EnePro Conference, Oulu Univ, Finland, pp 89–93
31. Marsh H, Rodríguez-Reinoso F (2006) Activated carbon. Elsevier, San Diego, pp 322–359
32. Hayashi J, Kazehaya A, Muroyama K, Watkinson AP (2000) Preparation of activated carbon from lignin by chemical activation. *Carbon* 38:1873–1878
33. Guo J, Lua AC (2002) Textural and chemical characterizations of adsorbent prepared from palm shell by potassium hydroxide impregnation at different stages. *J Colloid Interf Sci* 254:227–233
34. Adinata D, Ashri WM, Daud W, Aroua MK (2007) Preparation and characterization of activated carbon from palm shell by chemical activation with K_2CO_3 . *Bioresour Technol* 98:145–149
35. Lin YJ, Hwang GS (2009) Charcoal from biomass residues of a cryptomeria plantation and analysis of its carbon fixation benefit in Taiwan. *Biomass Bioenergy* 33:1289–1294
36. Lin YJ, Ho CL, Yu HY, Hwang GS (2008) Study on charcoal production with branches and tops wood of *Cryptomeria japonica* using an earthen kiln (in Chinese with English abstract). *Q J Chin For* 41:549–558
37. Lin SH, Wu SR, Wan HP, Hsu TW, Tsai YS, Chuang PH (2013) Application of bio-charcoal on the growth efficiency of *Mentha spicata* (in Chinese with English abstract). *Q J Chin For* 46:189–210
38. Kamikawa D, Kuroda K, Inoue M, Kubo S, Yoshida T (2009) Evaluation of combustion properties of wood pellets using a cone calorimeter. *J Wood Sci* 55:453–457
39. Yen YH, Chen CY, Wu KT, Tsai CJ, Liu SH (2011) The characteristics of torrefied agricultural and forest waste (in Chinese with English abstract). Republic of China centennial Seminar on sustainable management of forest resource. Natl Ilan Univ, Taiwan, pp 187–198
40. Díaz-Díez MA, Gómez-Serrano V, González CF, Cuerda-Correa EM, Macías-García A (2004) Porous texture of activated carbons prepared by phosphoric acid activation of woods. *Appl Surf Sci* 238:309–313
41. Ismadji S, Sudaryanto Y, Hartono SB, Setiawan LEK, Ayucitra A (2005) Activated carbon from char obtained from vacuum pyrolysis of teak sawdust: pore structure development and characterization. *Bioresour Technol* 96:1364–1369
42. Budinova T, Ekinici E, Yardim F, Grimm A, Björnbom E, Minkova V, Goranova M (2006) Characterization and application of activated carbon produced by H_3PO_4 and water vapor activation. *Fuel Process Technol* 87:899–905
43. Kumar BGP, Shivakamy K, Miranda LR, Velan M (2006) Preparation of steam activated carbon from rubberwood sawdust (*Hevea brasiliensis*) and its adsorption kinetics. *J Hazard Mater B* 136:922–929
44. Lin SH, Wu CC, Tsai IL (2007) Manufacturing powder activated carbon from Makino bamboo through processing with potassium salts (in Chinese with English abstract). *Q J Chin For* 40:81–95
45. Lin SH (2007) Manufacturing of powder activated carbon from Moso bamboo through potassium salts processing (in Chinese with English abstract). *Q J Chin For* 40:433–445
46. Chinese National Standard 10821 (1984) Method for determination of inherent moisture of coal and coke. Bureau of Standards, Metrology and Inspection, M. O. E. A., R. O. C, Taiwan
47. Chinese National Standard 10822 (1984) Method for determination of ash of coal and coke. Bureau of Standards, Metrology and Inspection, M. O. E. A., R. O. C, Taiwan
48. Chinese National Standard 10823 (1984) Method for determination of volatile matter of coal and coke. Bureau of Standards, Metrology and Inspection, M. O. E. A., R. O. C, Taiwan
49. Chinese National Standard 10824 (1984) Method for calculation of fixed carbon of coal and coke. Bureau of Standards, Metrology and Inspection, M. O. E. A., R. O. C, Taiwan
50. Chinese National Standard 697 (1965) Activated carbon powder, for industrial use. Bureau of Standards, Metrology and Inspection, M. O. E. A., R. O. C, Taiwan
51. Japanese Industrial Standards K 1474 (1991) Testing method for granular activated carbon. Japanese Standard Association, Tokyo, Japan
52. Wu WL, Wu SC, Lin HC (2010) Investigation on water activity and absorption properties of activated carbons prepared from corn cob, mushroom stalk and bagasse pith using methods of physical activation with CO_2 and steam (in Chinese with English abstract). *J Agric For Natl Chiayi Univ* 7:1–15
53. Barrett EP, Joyner LG, Halenda PH (1951) The determination of pore volume and area distribution in porous substances. I: computation from nitrogen isotherms. *J Am Chem Soc* 73:373–380
54. Hu Z, Srinivasan MP (1999) Preparation of high-surface-area activated carbons from coconut shell. *Microporous Mesoporous Mater* 27:11–18
55. Lin YJ, Liu CP, Lin JC (2002) Measurement of specific gravity and carbon content of important timber species in Taiwan (in Chinese with English summary). *Taiwan J For Sci* 17:291–299
56. Yang J, Qiu KQ (2009) Preparation of activated carbon by chemical activation under vacuum. *Environ Sci Technol* 43:3385–3390
57. Zhang J, Zhong Z, Shen D, Zhao J, Zhang H, Yang M, Li W (2011) Preparation of bamboo-based activated carbon and its application in direct carbon fuel cells. *Energy Fuels* 25:2187–2193
58. Rodríguez-Reinoso F, Molina-sabio M (1992) Activated carbons from lignocellulosic materials by chemical and/or physical activation: an overview. *Carbon* 30:1111–1118
59. Heschel W, Klose E (1995) On the suitability of agricultural by-products for the manufacture of granular activated carbon. *Fuel* 74:1786–1791
60. Williams PT, Reed AR (2006) Development of activated carbon pore structure via physical and chemical activation of biomass fibre waste. *Biomass Bioenergy* 30:144–152
61. McKee DW (1983) Mechanisms of the alkali metal catalyzed gasification of carbon. *Fuel* 62:170–175
62. Foo KY, Hameed BH (2012) Preparation, characterization and evaluation of adsorption properties of orange peel based activated carbon via microwave induced K_2CO_3 activation. *Bioresour Technol* 104:679–686
63. Foo KY, Hameed BH (2012) Mesoporous activated carbon from wood sawdust by K_2CO_3 activation using microwave heating. *Bioresour Technol* 111:425–432
64. Gregg SJ, Sing KSW (1982) Adsorption, surface area and porosity. Academic Press, London, pp 285–287